



HAL
open science

Stability and String Stability of Car-following Models with Reaction-time Delay

Guy Fayolle, Jean-Marc Lasgouttes, Carlos Flores

► **To cite this version:**

Guy Fayolle, Jean-Marc Lasgouttes, Carlos Flores. Stability and String Stability of Car-following Models with Reaction-time Delay. 2020. hal-03697661v6

HAL Id: hal-03697661

<https://inria.hal.science/hal-03697661v6>

Preprint submitted on 28 Apr 2020 (v6), last revised 17 Jun 2022 (v9)

HAL is a multi-disciplinary open access archive for the deposit and dissemination of scientific research documents, whether they are published or not. The documents may come from teaching and research institutions in France or abroad, or from public or private research centers.

L'archive ouverte pluridisciplinaire **HAL**, est destinée au dépôt et à la diffusion de documents scientifiques de niveau recherche, publiés ou non, émanant des établissements d'enseignement et de recherche français ou étrangers, des laboratoires publics ou privés.

Stability and String Stability of Car-following Models with Reaction-time Delay

Guy Fayolle, Jean-Marc Lasgouttes and Carlos Flores

Abstract

We investigate the transfer function emanating from the linearization of a car-following model, when taking into account a driver reaction time. This leads to nontrivial stability conditions, which are explicitly given. They are in particular satisfied whenever string stability holds. We also show how this reaction time can introduce a *partial string stability*, where the transfer function modulus remains smaller or equal to 1 up to some critical frequency. We explore conditions in the parameter space discriminating between the different regimes. This is a preliminary step of a forthcoming work about traffic stabilization via connected automated vehicles.

Index Terms

Stability of linear systems, modeling, traffic control, transportation networks, methods of the complex variable.

I. INTRODUCTION

It has been known for some time, and even demonstrated in the field [1], [2], that vehicles on a highway can suffer from stop-and-go traffic conditions without any external intervention. To explain this phenomenon, traffic evolution is studied at a microscopic level and further expanded as a series of interconnected systems named car-following models. These refer to the way drivers maintain a spacing gap towards the preceding vehicle. In other words, car-following models predict the motion of a human-driven vehicle in a vehicular stream, by studying the dynamics of the inter-vehicle gap.

Conceptualized for the first time by Pipes [3] and Reuschel [4], several car-following models have been proposed in the literature to simulate mathematically the driving behavior at a microscopic

Guy Fayolle and Jean-Marc Lasgouttes are with RITS project-Team, Inria, *firstname.lastname@inria.fr*.

Carlos Flores is with California PATH program of the Institute of Transportation Studies, UCB, *carfloresp@berkeley.edu*

level. The review of car-following models in [5] highlights five groups: Gazis-Herman-Rothery (GHR, also known as GM model), collision-avoidance models, linear models, psycho-physical or action-point models and fuzzy logic-based models.

Over the years, the aforementioned models served as a basis for more complex and accurate models. The Gipps' car-following model [6], has been widely used, both in research and practice for its accuracy. Later, Treiber *et al.* [7] introduced the *Intelligent Driver Model* (IDM) which gained a lot of attention, becoming the most popular car-following model for human drivers. In [8], IDM was extended to take into account driver's adaptation effect using memory functions. More recently, IDM+ has been proposed for traffic flow study [9].

Several studies added that reaction-time delays of the human driver should be considered to represent more accurately upstream wave propagation in a traffic lane. For instance, stop-and-go traffic jams have been shown to be connected to these delays in [10], [11], [12], demonstrating that an unexpected deceleration of the front vehicle is followed by an even stronger ego-deceleration to avoid rear-end collision. This amplification of vehicle states along a string can lead to a traffic jam. An analysis of such a delayed car-following model on a circle can be found in [13].

Several authors [14], [15], [16] have suggested that it is possible to use a small proportion of automated vehicles to regulate the traffic. These studies are set in a traffic regime which exhibits string instability, which means in terms of transfer function that any excitation of a frequency below a certain limit is amplified. We are interested here in a slightly different setting, where reaction time is taken into account for human drivers. In this case, we show that the system may be unstable under some conditions, but also that there is an interesting regime where string instability only concerns frequencies in a particular band.

This paper is intended as a foundation of a larger work on traffic stabilization by means of a fleet of cooperative automated vehicles. However, contrary to the work in [14], our approach is based on a car-following model with reaction-time delay, rather than on a first order fluid model. The continuation of these studies will concern shockwave analysis and adequate traffic-stabilizing control strategies.

The paper is organized as follows: after describing the model in Section II, the stability domain of the linearized version is given in Section III as well as its relation to string stability in Section IV. We introduce the notion of partial string stability, which is of interest for our traffic stabilization vision, in Section V and provide different conditions under which it can take place. Section VI is devoted to numerical computation in the case of IDM, which shows in which range

of parameters one can expect partial string stability to take place. Finally, Section VII discusses control strategies made possible by partial string stability and further work on the subject.

II. THE MODEL

We start from a classical *car-following model* on a line with identical vehicles, in which we introduce a reaction time τ for each driver. For simplicity of presentation, we follow the notation and the development of [16]. Let $x_j(t)$ be the position of vehicle j along the road at time t , $v_j(t)$ its speed and $a_j(t)$ its acceleration. We assume that vehicle j obeys a car-following model of the form

$$\begin{aligned} a_j(t + \tau) &= f(x_{j-1}(t) - x_j(t), v_{j-1}(t) - v_j(t), v_j(t)) \\ &\stackrel{\text{def}}{=} f(\Delta x_j(t), \Delta v_j(t), v_j(t)). \end{aligned} \quad (1)$$

The acceleration at time t is thus a function f of the following variables, delayed by τ : the distance to the vehicle in front, their relative speed and the speed of vehicle j itself. A typical example of such a car-following model is the Intelligent Driver Model (IDM) [17], which we will use in our examples.

The relation at equilibrium between the heading Δx^* and the speed v^* is given by the equation

$$0 = f(\Delta x^*, 0, v^*). \quad (2)$$

The linearization of (1) at point $(\Delta x^*, 0, v^*)$ yields

$$a_j(t + \tau) = k_{dx}(\Delta x_j(t) - \Delta x^*) + k_{dv}\Delta v_j(t) + k_v(v_j(t) - v^*), \quad (3)$$

where the parameters k_{dv}, k_{dx}, k_v are positive and stand for the following partial derivatives at equilibrium

$$k_{dx} = \frac{\partial f}{\partial \Delta x}, \quad k_{dv} = \frac{\partial f}{\partial \Delta v}, \quad k_v = -\frac{\partial f}{\partial v}.$$

Equation (3) defines a second-order linear differential equation for the positions of the vehicles. For all $\Re(s) \geq 0$, let $V_j(s)$ denote the Laplace transform of $v_j(t) - v^*$. Then the fundamental transfer function takes the form

$$U(s) \stackrel{\text{def}}{=} \frac{V_j(s)}{V_{j-1}(s)} = \frac{k_{dv}s + k_{dx}}{s^2 e^{s\tau} + (k_{dv} + k_v)s + k_{dx}}, \quad \Re(s) \geq 0, \quad (4)$$

Note that, unlike in [16], $U(s)$ is no more a rational but a transcendental function, because of the term e^{sT} . As we shall see in the next sections, the analysis and the behavior of the system become more intricate.

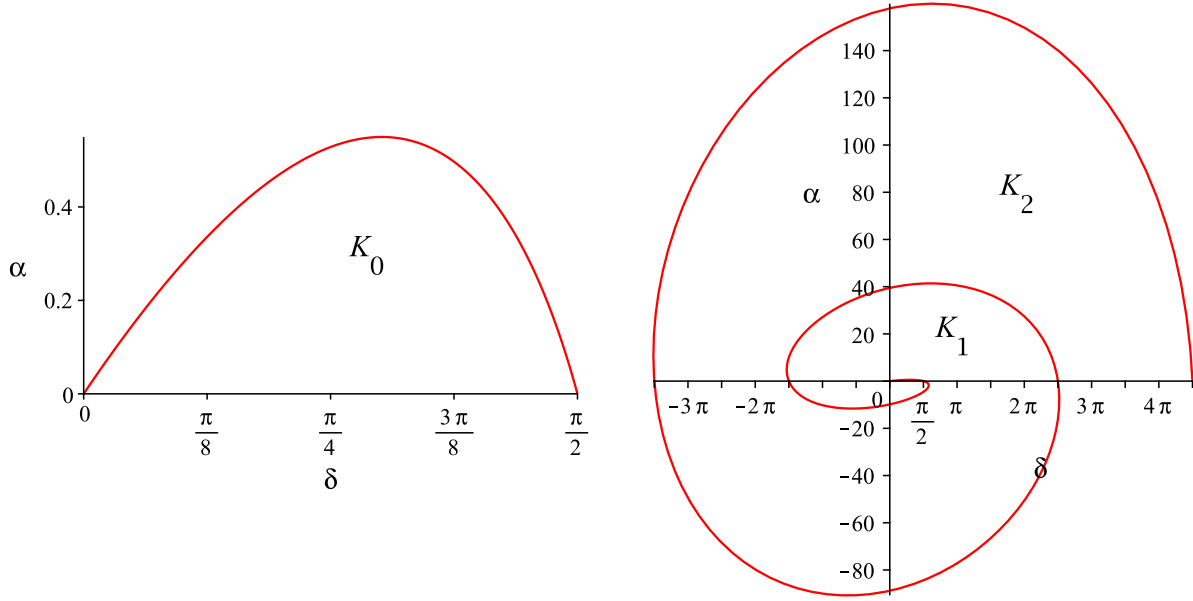


Fig. 1. Left: stability region in terms of the parameters α and δ . Right: the spiral (7) represented for $y \in [0, \frac{9\pi}{2}]$; note that the stability region K_0 of the left panel is barely visible in the display of the right panel.

III. STABILITY REGION

The first basic question about the dynamics of (3) concerns its stability.

Definition III.1 (Stability). *The system is stable if and only if $U(s)$ has no pole in the region $\Re(s) \geq 0$.*

The physical meaning of this property is that a finite perturbation of x_i should never have an unbounded effect. Note that stability always holds when $\tau = 0$ as in [15], [16].

Let us analyze the poles of $U(s)$ in the region $\Re(s) \geq 0$. For this purpose, it will be convenient to introduce the scaling

$$z = s\tau, \quad \alpha = \tau^2 k_{dx}, \quad \beta = \tau k_{dv}, \quad \gamma = \tau k_v, \quad \delta = \beta + \gamma. \quad (5)$$

Then (4) can be rewritten as

$$U(z) = \frac{\beta z + \alpha}{D(z)}, \quad \text{where } D(z) = z^2 e^z + \delta z + \alpha. \quad (6)$$

We state now necessary and sufficient conditions for the system to be stable. They are nontrivial due the presence of the reaction time τ . Interestingly, they only depend on α and $\delta = \beta + \gamma$, but not on the individual values of β and γ .

The function $D(z)$ belongs to the class of exponential polynomials. A lot of works have been devoted to the zeros of these polynomials (see e.g. [18]). Although a part of the next theorem follows directly from [18, section 13.9], we propose a new self-contained proof of the stability conditions, the method being applicable to more general transfer functions.

Theorem III.2. *In the (δ, α) plane, let \mathcal{L} be the curve shown in Fig. 1 and represented in the parametric form*

$$\begin{cases} \delta = y \sin y, \\ \alpha = y^2 \cos y, \end{cases} \quad y \geq 0. \quad (7)$$

Then the system is stable if and only if the couple of parameters (α, δ) belongs to the finite domain K_0 , bounded by the curve \mathcal{L} and the open segment $]0, \pi/2[$ on the δ -axis.

In the positive quarter plane (δ, α) , define K_j , the j -th positive sector of \mathcal{L} , as the domain corresponding in (7) to $y \in [0, \pi/2] + 2j\pi$, $j \geq 0$, see Fig. 1. Then, when $(\delta, \alpha) \in K_j$, the function $D(z)$ has exactly $2j$ conjugate zeros with positive real parts.

In addition, the set of equations (7) is equivalent to the algebraic differential equation

$$\frac{d\alpha}{d\delta} = \frac{4\alpha - \delta(\delta^2 + \sqrt{\delta^4 + 4\alpha^2})}{2(\alpha + \delta)}, \quad (8)$$

subject to the initial conditions $\alpha(0) = 0$ with $\alpha'(0) = 1$.

A clear consequence of this result is that, when the parameters (α, δ) do not belong to K_0 , the system is *unstable*.

Proof. We want to find conditions ensuring the existence of zeros for the function D in the right half-plane $\Re(z) \geq 0$. The main ingredient will be a proper use of Rouché's theorem, together with an argument of continuity with respect to the parameters (δ, α) .

First consider the imaginary axis $\{z = iy, y \in \mathbb{R}\}$, where D may have two possible zeros at the points iy_0 and $-iy_0$, which are the real solutions of the system

$$\begin{cases} y^2 \cos y = \alpha, \\ y \sin y = \delta, \end{cases}$$

which coincides exactly with (7). When y_0 exists, it is immediate to check that, necessarily,

$$y_0 = \left(\frac{\delta^2 + \sqrt{\delta^4 + 4\alpha^2}}{2} \right)^{\frac{1}{2}} > \delta. \quad (9)$$

Viewing in (7) the variables y and α as functions of δ , one gets by differentiation

$$\begin{cases} \frac{dy_0}{d\delta}(2y_0 \cos y_0 - y_0^2 \sin y_0) = \frac{d\alpha}{d\delta}, \\ \frac{dy_0}{d\delta}(\sin y_0 + y_0 \cos y_0) = 1, \end{cases}$$

so that

$$\frac{d\alpha}{d\delta} = \frac{2\alpha - \delta y_0^2}{\alpha + \delta},$$

which is exactly equivalent to (8) by using (9).

It is important to observe that the differential equation (8) has the classical form

$$\frac{d\alpha}{d\delta} = F(\delta, \alpha), \quad \forall (\delta, \alpha) \in \Delta \in \mathbb{R}^{+2},$$

where Δ is a finite domain including the point $(0, 0)$, where $F(\delta, \alpha)$ is not continuous, and nor does satisfy a classical Lipschitz condition with respect to α .

On the other hand, whenever system (7) holds, we have the immediate following results.

1. $\alpha'(0) = \lim_{\delta \rightarrow 0} \frac{\alpha}{\delta} = 1$.
2. If $\alpha = 0$, then either $\delta = 0$ or $\delta = \frac{\pi}{2} + 2k\pi$, for any integer $k \geq 0$.
3. If $\delta = 0$, then $\alpha = (2\ell\pi)^2$, for any integer $\ell \geq 0$.

The curve \mathcal{L} , which is parametrized by (7), looks like an Archimedean spiral, the spires of which are dilated along the α -axis in the (δ, α) -plane.

In the course of the proof, we shall use the so-called Rouché's theorem, which we recall for the sake of completeness.

Theorem (Rouché, see e.g. [19]). *For any two complex-valued functions f and g holomorphic inside some region \mathcal{H} with simple closed contour $\partial\mathcal{H}$, if $|g(z)| < |f(z)|$ on $\partial\mathcal{H}$, then f and $f + g$ have the same number of zeros inside \mathcal{H} , where each zero is counted with its multiplicity.*

a) Proof of stability.: The baseline of reasoning will be, *starting with convenient small values for (α, δ) , to apply the above theorem to the functions $f(z) = z^2 e^z + \delta z$ and $g(z) = \alpha$ (constant) on a properly chosen contour, and then to proceed by continuity with respect to the parameters (δ, α) .*

In the right half-plane, consider the closed contour $C(\delta, R)$ consisting of the two semicircles centered at the origin of respective radii R and δ , plus the two segments of the imaginary axis $[i\delta, iR]$ and $[-iR, -i\delta]$ respectively. Henceforth, R will stand for a large positive number.

Lemma III.3. For all (α, δ) in the region $0 < \alpha < \delta^2 < 1/4$, the following inequality holds.

$$|z^2 e^z + \delta z| > \alpha, \quad \forall z \in C(\delta, R). \quad (10)$$

Proof. Inequality (10) is evidently satisfied for z on the semicircle of radius R . The situation for the remaining components of the contour is twofold.

(i) $z \in [i\delta, iR] \cup [-iR, -i\delta]$. Setting $z = iy$, y real,

$$|ze^z + \delta|^2 = y^2 - 2\delta y \sin y + \delta^2 \geq (1 - 2\delta)y^2 + \delta^2 > \delta^2$$

(ii) z belongs to the semicircle of radius δ , that is $z = \delta e^{i\theta}$, $-\pi/2 \leq \theta \leq \pi/2$. Setting $Y \stackrel{\text{def}}{=} e^{\delta \cos \theta} \geq 1$, we get directly

$$|ze^z + \delta|^2 = \delta^2 [Y^2 + 2Y \cos(\theta + \delta \sin \theta) + 1]. \quad (11)$$

By the monotony of the sine and cosine functions, we have

$$\cos(\theta + \delta \sin \theta) > \cos(\pi/2 + \delta) = -\sin \delta, \quad \forall \theta \in [0, \pi/2],$$

and (11) yields

$$|ze^z + \delta|^2 > 2\delta^2(1 - \sin \delta).$$

Finally, for $0 < \alpha < \delta^2 < 1/4$, (10) holds everywhere on $C(\delta, R)$, and the lemma is proved. \square

In a second step, we shall show in addition that $D(z)$ has no zeros in the closed domain bounded by the half-disk $z = \delta e^{i\theta}$, $\theta \in [-\pi/2, \pi/2]$ in the right half-plane.

Lemma III.4. For all $\alpha > \delta^2(e^{2\delta} - 1)^{1/2}$, the equation

$$z^2 e^z + \delta z + \alpha = 0$$

has no roots in the half-disk $z = \rho e^{i\theta}$, $0 \leq \rho \leq \delta$ and $\theta \in [-\pi/2, \pi/2]$.

Proof. By Rouché's theorem, it suffices to establish on the contour of this half-disk the inequality

$$|\delta z + \alpha| > |z^2 e^z|. \quad (12)$$

Letting $z = x + iy$, we analyze separately the two components of the domain.

(i) On the diameter of the half-disk, $x = 0$ and

$$|\delta z + \alpha|^2 - |z^2 e^z|^2 = \delta^2 y^2 + \alpha^2 - y^4 > 0, \quad 0 \leq |y| \leq \delta,$$

which shows (12).

(ii) $z = \delta e^{i\theta}$, $\theta \in [-\pi/2, \pi/2]$. Here,

$$|\delta z + \alpha|^2 = \delta^4 + 2\alpha\delta x + \alpha^2, \quad \text{and} \quad |z^2 e^z|^2 = \delta^4 e^{2x}.$$

Now, as $x \geq 0$, (12) will clearly be satisfied by choosing for instance

$$\alpha^2 > \delta^4(e^{2\delta} - 1),$$

and the proof of the lemma is terminated. \square

Putting together the results of Lemmas III.3 and III.4, we can conclude that $D(z)$ has no zeros in the right half-plane for the parameter region

$$\left\{ \delta^2(e^{2\delta} - 1)^{1/2} < \alpha < \delta^2 < \frac{(\log 2)^2}{4} \right\},$$

which lies clearly in the interior of the domain K_0 .

On the other hand, by the principle of the argument (see e.g, [20]), the number of zeros of $D(z)$ can be expressed by means of a Cauchy type integral of the form

$$\frac{1}{2i\pi} \int_{\mathcal{U}} \frac{D'(t)}{D(t)} dt,$$

\mathcal{U} being the boundary of the semicircle of radius R in the right half-plane. *This integral takes integer values and is continuous with respect to (δ, α) , as long as $D(z)$ does not vanish on the contour. For large R , this can occur only on the imaginary axis, implying*

$$D(iy) = (\alpha - y^2 \cos y) + iy(\delta - y \sin y) = 0, \quad y \in \mathbb{R},$$

which is equivalent to (7). Hence in the interior of K_0 , $D(z)$ has no zeros, and the stability part of the theorem is proved.

b) The zeros of $\mathcal{D}(z)$ for the parameter domain K_j , $j \leq 1$.: In the parameter space, take a point $P = (\delta, \alpha) \geq (0, 0)$ located inside K_j and let P move to the boundary of K_j , to enter K_{j+1} , so that system (7) holds, which means that two zeros of $D(z)$ appear on the imaginary axis in the z -plane. These conjugate zeros come from the left half-plane and all what we have to show is that their real part becomes strictly positive when P switches from K_j to K_{j+1} . We deal with the case $j = 0$, the argument being the same for all j .

Let P reach the boundary of K_0 to enter K_1 via the point $(\pi/2, 0)$, and suppose for a while that α is an arbitrary positive function of δ , locally differentiable around $\delta = \pi/2$, with a derivative $q \stackrel{\text{def}}{=} \alpha'(\pi/2) > -\pi^2/4$ (the value of the slope of the curve \mathcal{L} at $\delta = \pi/2$) to ensure that the point $P = (\pi/2 + \varepsilon, \varepsilon q)$ belongs to K_1 for ε sufficiently small.

Then the possible zeros of $D(z)$ are locally differentiable with respect to δ around $\delta = \pi/2$, whence, by taking the derivative of $D(z) = 0$ and writing $z'(\delta) = \frac{dz}{d\delta}$,

$$z'(\delta)[ze^z(z+2) + \delta] + z + \alpha'(\delta) = 0. \quad (13)$$

Instantiating $\delta = \pi/2$ in (13), we have $z = \pm i\pi/2$. Choosing for example $z = i\pi/2$, we obtain

$$z'(\pi/2) = \frac{q + i\pi/2}{\pi(1 + i\pi/4)} = \frac{q + \pi^2/4 + i\pi(1 - q)/4}{\pi(1 + \pi^2/4)},$$

and the real part of $z'(\pi/2)$ is positive as soon as $q + \pi^2/4 > 0$. Thus, when the point P enters K_1 , two conjugate zeros of $D(z)$ come into the right complex half-plane.

A similar phenomenon occurs when P passes from K_j to K_{j+1} , creating two additional zeros of $D(z)$ in the right.

The proof of the theorem is terminated. □

Remark III.5. *We always assumed $\alpha > 0$. For the sake of completeness, let us briefly analyze the case $\alpha = 0$, although it is of little physical interest, since it implies $k_{dx} = 0$.*

Here, by (6), we are left with the analysis of the simpler equation

$$ze^z + \delta = 0,$$

the general solution of which is $W(-\delta)$, the special Lambert W -function, see e.g. [21]. $W(z)$ has an infinite number of branches classically denoted by $W(k, z)$, k integer, and exactly one of them, $W(0, w)$, is analytic around the origin and given by

$$W(0, w) = \sum_{n=1}^{\infty} \frac{(-n)^{n-1} w^n}{n!},$$

where the series is convergent for $|w| \leq e^{-1}$. In particular, $W(0, -\delta)$ does not vanish in the interior of the disk of radius e^{-1} .

The curves separating the branches are

$$\{-y \cot y + iy : 2k\pi < \pm y \leq (2k+1)\pi\}, \quad \text{for } k \geq 1.$$

These curves form the images of the negative real axis under the branches $W(k, z)$. As in the case $\alpha > 0$, we have

$$\Re[W(k, -\delta)] < 0, \quad 0 < \delta < \pi/2, \quad \forall k = 0, \pm 1, \dots,$$

and $U(z)$ has no poles for $\delta \in [0, \pi/2]$.

IV. STRING STABILITY

Even if the system is stable, another phenomenon may occur, when, for some $y \in \mathbb{R}$, $|U(iy)| > 1$: indeed, in this case, since

$$V_j(iy) = U^n(iy)V_{j-n}(iy), \quad \forall 1 \leq j \leq n,$$

it appears that small perturbations could be amplified as they propagate in upstream direction. A metric has been introduced in the literature that relates on how systems' states energy is propagated element-wise in a string of systems. It is referred as *string stability* [22], [23].

Definition IV.1 (String stability). *The system is called string stable if and only if $|U(iy)| \leq 1$ for all $y \in \mathbb{R}$.*

Theorem IV.2. *String stability implies stability, that is $(\delta, \alpha) \in K_0$.*

Proof. Assume for some parameter region (α, δ, β) string stability holds. This is equivalent to say that, for $z = iy$ on the imaginary axis,

$$|D(iy)| > |\alpha + i\beta y|, \quad y \geq 0.$$

Choose $R > 0$ sufficiently large such that

$$|D(z)| > |\beta z + \alpha|, \quad \forall |z| \geq R.$$

Then $D(z)$ and $D(z) - (\beta z + \alpha) \stackrel{\text{def}}{=} E(z) = z(ze^z + \gamma)$ have, by Rouché's theorem, the same number of zeros in the closed region \mathcal{V} bounded by the curve \mathcal{U} introduced in the stability proof of Theorem III.2.

Note that, for all $z = x + iy, x \geq 0$, we have

$$\Re[D(z)] = \Re[E(z)] + \beta x + \alpha,$$

showing that the point of affix $D(z)$ lies always to the right of $E(z)$.

Proceeding now as in the proof of Theorem III.2 (details are omitted), it is easy to see that $E(z)/z$ has no zeros in the region \mathcal{V} from which we remove a small semicircle of radius $\gamma + \varepsilon$, centered at the origin and located in the right half-plane, where ε is an arbitrary small positive number. Hence, $D(z)$ cannot vanish in \mathcal{V} , since this would contradict the equality of the number of zeros in the region \mathcal{V} . The theorem is proved. \square

V. PARTIAL STRING STABILITY

String stability is easy to investigate when the reaction time is $\tau = 0$: either it holds, or $|U(iy)| \geq 1$ in a neighborhood of 0. When $\tau > 0$, there is another possible situation, that we introduce as *partial string stability*.

Definition V.1 (Partial string stability). *The system is partially string stable if and only if there exists $y_c > 0$ such that $|U(iy)| \leq 1$ for all $|y| \leq y_c$.*

Partial string stability covers cases where $|U(iy)|$ can be greater than 1 for some $|y| > y_c$. Accordingly, the next step will be to analyze the modulus of $U(z)$ on the imaginary axis, especially its position with respect to the value 1. As the reader will note, finding exact necessary and sufficient conditions for string stability in the parameter domain is a thorny problem, which we intend to tackle hereafter.

A. Necessary conditions for partial string stability

In the next theorem, we give in particular the maximum interval containing all possible frequencies y satisfying $|U(iy)| = 1$.

Theorem V.2. *The following properties hold.*

(i) *The system can be string stable or partially string stable only if*

$$2\alpha < \delta^2 - \beta^2 \stackrel{\text{def}}{=} \mu, \quad (14)$$

and this condition implies also stability if $\delta < a \sin a \approx 1.04098$, where $a = \arccos(\sqrt{2} - 1)$.

(ii) *The system is string stable if*

$$2\alpha < \mu \quad \text{and} \quad \delta < \frac{1}{2}. \quad (15)$$

(iii) *Assuming condition (14), any critical y_c such that $|U(iy_c)| = 1$ satisfies the inequalities*

$$\sqrt{Y_-} < y_c < \sqrt{Y_+}, \quad \text{with } Y_{\pm} = \beta^2 + \delta^2 \pm 2\sqrt{\beta^2\delta^2 + \alpha^2}. \quad (16)$$

One can check that condition (14) does not depend on $\tau > 0$ and is the same as condition (10) in [15], where $\tau = 0$, in which case (14) is actually necessary and sufficient for string stability.

Proof. For the sake of shortness, let $F(y) \stackrel{\text{def}}{=} |U(iy)|$. Then an easy algebra yields

$$F(0) = 1, \quad F'(0) = 0, \quad F''(0) = \frac{2(2\alpha - \mu)}{\alpha^2}.$$

In addition,

$$\frac{1 - F(y)}{y^2} = \frac{G(y)}{|D(iy)|^2},$$

where

$$G(y) \stackrel{\text{def}}{=} y^2 - 2(\delta y \sin y + \alpha \cos y) + \mu, \quad (17)$$

and now (14) becomes immediate from

$$\lim_{y \rightarrow 0} \frac{1 - F(y)}{y^2} = -\frac{F''(0)}{2} = \frac{\mu - 2\alpha}{\alpha^2}.$$

The condition $\mu > 2\alpha$, rewritten as $\delta^2 > \beta^2 + 2\alpha$, implies $\delta^2 > 2\alpha$, in which case the couple (δ, α) lies inside the domain K_0 defined in Theorem III.2. By using (7), one checks easily that, in the parameter space, the parabola $\alpha = \delta^2/2$ crosses the curve \mathcal{L} when

$$\begin{aligned} y^2 \sin^2 y = 2y^2 \cos y &\iff \cos^2 y + 2 \cos y - 1 = 0 \\ &\iff y = \arccos(\sqrt{2} - 1), \end{aligned}$$

which gives $\delta = y \sin y \approx 1.04098$, showing property (i).

On the other hand, since, for all $y > 0$,

$$G(y) = y(y - 2\delta \sin y) + \mu - 2\alpha \cos y > y^2(1 - 2\delta) + \mu - 2\alpha,$$

equation (17) has no real root if $\{\delta < 1/2\} \wedge \{\mu > 2\alpha\}$, proving (15) and (ii).

As for (iii), we note first

$$G(0) = \mu - 2\alpha, \quad G'(0) = 0, \quad G''(0) = 2(1 + \alpha - 2\delta).$$

One could think that the curvature of G at the origin (i.e. the sign of $G''(0)$) plays a decisive role in the way $F(y)$ reaches and exceeds 1. Actually, it will emerge in the sequel that this is not the case.

It is worth illustrating on a toy example the existence of a set of positive parameters α, β, γ , for which $F(y)$ becomes strictly larger than 1 for some y . Taking for instance $y = \pi/4$, one can check that the quantity

$$G(\pi/4) = \gamma^2 + \left(2\beta - \frac{\pi\sqrt{2}}{4}\right)\gamma + \frac{\pi^2}{4} - \sqrt{2}\left(\frac{\beta\pi}{4} + \alpha\right)$$

can be rendered negative for $\beta = \frac{\pi}{\sqrt{2}}$, $(\gamma, \alpha) \in [0, \gamma_0] \times [0, \alpha_0]$, the constraint $\mu > 2\alpha$ being satisfied in these intervals.

The problem of the existence of y_c in (16) can be formulated in terms of the intricate following puzzle.

For given parameters α, β, γ , find the conditions ensuring the existence of y_c , the smallest positive root of $G(y) = 0$, where $G(y)$ was defined by equation (17).

To this end, let us introduce the family of parametrized trinomials $H(y, z)$, where z stands for a positive real parameter, and

$$H(y, z) = y^2 - 2\delta y \sin z - 2\alpha \cos z + \mu. \quad (18)$$

Setting $t = \tan(z/2)$ and using the classical formulas

$$\sin z = \frac{2t}{1+t^2}, \quad \cos z = \frac{1-t^2}{1+t^2},$$

one checks easily that the equation $H(y, z) = 0$ corresponds in a one-to-one way to the function $K(y, t) = 0$, where

$$\begin{aligned} K(y, t) &= (y^2 + 2\alpha + \mu)t^2 - 4\delta ty + y^2 - 2\alpha + \mu \\ &= (1+t^2)y^2 - 4\delta ty + (\mu + 2\alpha)t^2 + \mu - 2\alpha. \end{aligned} \quad (19)$$

In the sequel $K(y, t)$ will be viewed, *ad libitum*, either as a trinomial in y or a trinomial in t .

Hence, $G(y) \equiv H(y, y) = 0$ is plainly equivalent to the system

$$\begin{cases} K(y, t) = 0, \\ t = \tan(y/2). \end{cases} \quad (20)$$

Since $G(y)$ is an even function of y , we shall only look for its positive roots, remarking that if (y, t) satisfies (20), then $y > 0 \Rightarrow t > 0$. This means that we can restrict ourselves to the roots of G of the form $y = y_1 + 2k\pi$ with $0 < y_1 < \pi$ and $k \geq 0$.

In the sequel, at our convenience, we shall use the variables $Y \stackrel{\text{def}}{=} y^2$ and $T \stackrel{\text{def}}{=} t^2$. Also, according to (14), it is worth recalling that $\mu = \delta^2 - \beta^2$.

The reduced discriminant of $K(y, t) = 0$, considered as a quadratic equation in t , is equal to

$$A(Y) \stackrel{\text{def}}{=} -Y^2 + 2(2\delta^2 - \mu)Y + 4\alpha^2 - \mu^2, \quad (21)$$

which has two real positive roots Y_+, Y_- , where

$$Y_- = \beta^2 + \delta^2 - 2\sqrt{\beta^2\delta^2 + \alpha^2}, \quad Y_+ = \beta^2 + \delta^2 + 2\sqrt{\beta^2\delta^2 + \alpha^2}. \quad (22)$$

Quite similarly, the reduced discriminant of $K(y, t) = 0$, considered now as a quadratic equation in y , is equal to

$$B(T) \stackrel{\text{def}}{=} -(2\alpha + \mu)T^2 + 2(2\delta^2 - \mu)T + 2\alpha - \mu, \quad (23)$$

which has two real positive roots T_+, T_- , where

$$T_- = \frac{Y_-}{2\alpha + \mu}, \quad T_+ = \frac{Y_+}{2\alpha + \mu}.$$

Hence, any possible positive solution (y, t) of (20) necessarily satisfies the inequalities

$$\sqrt{Y_-} \leq y \leq \sqrt{Y_+}, \quad \sqrt{T_-} \leq t \leq \sqrt{T_+}, \quad (24)$$

since in this case $A(Y)$ and $B(T)$, respectively given by (21) and (23), are positive, which proves in particular (16) and the theorem. \square

Remark V.3. *On the other hand, by using the elementary inequalities*

$$y - y^3/6 \leq \sin y \leq y, \quad 1 - y^2/2 \leq \cos y \leq 1 - y^2/2 + y^4/24,$$

we get the following easy bounds, valid for all $y > 0$,

$$\frac{\delta}{3}y^4 \geq G(y) - (1 + \alpha - 2\delta)y^2 + 2\alpha - \mu \geq -\frac{\alpha}{12}y^4,$$

offering practical help to find concrete sufficient conditions for the existence of real zeros of G .

B. About a surface in the parameter domain ensuring partial string stability

From now on, we assume that the system is stable and that condition (14) holds. To characterize the exact parameter regions ensuring the existence of positive roots for equation (17), we propose two directions, both of them having a geometrical flavor.

a) Intersection of a quartic curve with a tangent curve.: Finding the exact necessary and sufficient conditions for string stability is tantamount to locate the closed curve $\{K(y, t) = 0\}$ with respect to the periodic curve $\{t = \tan(y/2)\}$, in the region defined by (24) in the (y, t) -plane. In particular, one must specify their possible tangency points, obtained by means of the additional relation

$$\frac{\partial K(y, t)}{\partial t} + \frac{d \tan(y/2)}{dy} = 0,$$

which, by using the identity

$$\frac{d \tan(y/2)}{dy} = \frac{1 + t^2}{2},$$

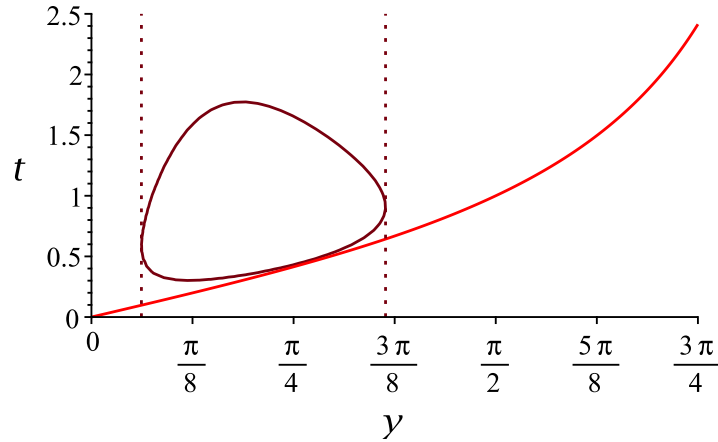


Fig. 2. Representation of $K(x, t) = 0$ and $t = \tan(y/2)$ for arbitrary parameter values $\alpha = 0.074$, $\beta = 0.45$ and $\gamma = 0.235$, chosen so that the curves are tangent. The vertical dotted lines mark the bounds (16).

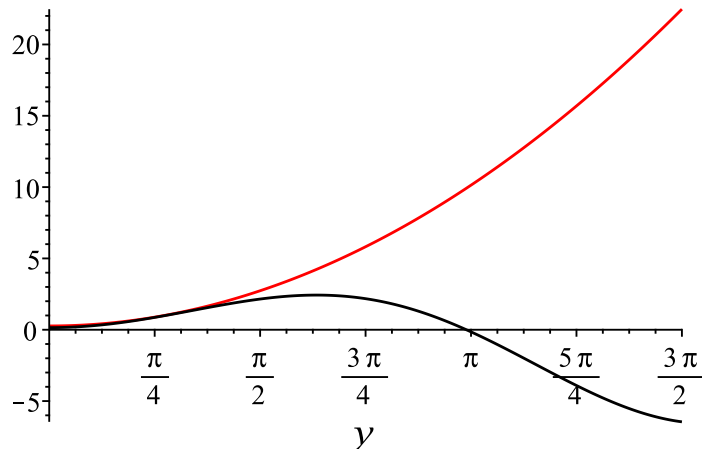


Fig. 3. The two functions defined in (26), for the same parameter values as in Fig. 2.

yields the algebraic equation

$$t(1 + t^2)y^2 + 2(1 - \delta)(t^2 + 1)y + (2\alpha + \mu)t(1 + t^2) - 4\delta t = 0. \quad (25)$$

The system made by (20) and (25) contains three equations with only two unknowns, and therefore there exists a relationship between the parameters (α, δ, μ) , actually a *surface* allowing to discriminate between existence and non existence of solutions. However, the related algebra as well as numerical implementations are rather tedious, and this question remains a pending issue, see Fig. 2.

b) *Intersection of a parabola with a linear-sinusoidal curve.*: Here the idea is to analyze the first possible tangency point in the (y, z) -plane of the two curves (see Fig. 3)

$$\begin{cases} z = y^2 + \mu, & (\text{parabola}) \\ z = 2(\delta y \sin y + \alpha \cos y). \end{cases} \quad (26)$$

By identifying the normal vectors at the contact point of the two curves, we immediately obtain the following system

$$\begin{cases} \delta y \cos y + (\delta - \alpha) \sin y = y, \\ 2(\alpha \cos y + \delta y \sin y) = y^2 + \mu, \end{cases} \quad (27)$$

which in turn gives

$$\begin{cases} \cos y = \frac{(\alpha + \delta)y^2 + \mu(\alpha - \delta)}{2[\delta^2 y^2 + \alpha(\alpha - \delta)]}, \\ \sin y = \frac{\delta y^3 + (\mu\delta - 2\alpha)y}{2[\delta^2 y^2 + \alpha(\alpha - \delta)]}. \end{cases} \quad (28)$$

System (28) produces the following third degree equation in $Y = y^2$, namely

$$\begin{aligned} & \delta^2 Y^3 + [(\alpha - \delta)^2 + 2\delta^2(\mu - 2\delta^2)]Y^2 \\ & + [2(\mu - 4\delta^2 + 2)\alpha^2 + 4\alpha\delta(2\delta^2 - \mu) + \delta^2\mu(\mu - 2)]Y \\ & + (\delta - \alpha)^2(\mu^2 - 4\alpha^2) = 0, \end{aligned} \quad (29)$$

the convenient root of which (in a sense to be made precise below) will be denoted by $Y_m = y_m^2$.

The discriminant of (29) is equal to

$$\Delta = 16 W (\alpha^2 + \delta^4 - \delta^2\mu)(\alpha^2 + \alpha\delta - \delta^2\mu)^2, \quad (30)$$

where W is the following polynomial of degree 2 with respect to μ

$$\begin{aligned} W &= \delta^2(\delta^2 - 1)\mu^2 \\ &- [12\delta^4 - 10\alpha\delta^3 + (2\alpha^2 - 11)\delta^2 + 8\alpha\delta - \alpha^2]\mu \\ &+ 16\delta^6 - 16\alpha\delta^5 - 8\delta^4 - 4\alpha\delta^3 \\ &+ (25\alpha^2 + 1)\delta^2 - (10\alpha^2 + 6)\alpha\delta + \alpha^2(\alpha^2 + 1). \end{aligned}$$

Since $\mu = \delta^2 - \beta^2$, the two explicit factors in (30) are nonnegative, so that Δ and W have the same sign.

From condition (14), the product of the roots in (29) is negative and there always exists a negative root which is of course not admissible.

- If $W < 0$, (29) has no admissible solution.
- If $W \geq 0$, (29) has three real roots. Then, either they are all negative and there is no admissible solution, or two of them are positive and the issue is to select the correct one.

It might be useful to note that the discriminant of the quadratic polynomial W takes the simple form

$$\Delta_W = (\alpha - \delta)(4\delta^3 - 5\delta + \alpha)^3,$$

noting that, for all $(\alpha, \delta) \in K_0$, we have $\delta \geq \alpha$ by (7).

Clearly, for $(\alpha, \delta) \in K_0$ and δ satisfying (15), $W = 0$ represents a *necessary separating surface* S_1 in the parameter domain (α, δ, μ) : on one side of S_1 , G defined in (17) may have real zeros, while it has none on the other side.

To proceed further, we fix δ and consider μ and y_m as functions of the variable α . Then, upon combining the first equation of (27) with (28), we get

$$\begin{aligned} \frac{dy_m}{d\alpha} &= \frac{\sin y_m}{(2\delta - \alpha) \cos y_m - \delta y_m \sin y_m - 1} \\ &= \frac{-y_m(\delta y_m^2 + \mu\delta - 2\alpha)}{\delta^2 y_m^4 + (\mu\delta^2 + \alpha^2 - 3\alpha\delta)y_m^2 + ((\mu + 2)\alpha - 2\delta\mu)(\alpha - \delta)}. \end{aligned} \quad (31)$$

Similarly, after some algebra (!), the second equation of (27), allied with (31), gives

$$\begin{aligned} \frac{d\mu}{d\alpha} &= 2[y_m(\delta \cos y_m - 1) + (\delta - \alpha) \sin y_m] \frac{dy_m}{d\alpha} + 2 \cos y_m \\ &= \frac{(\alpha + \delta)Y_m + \mu(\alpha - \delta)}{\delta^2 Y_m + \alpha(\alpha - \delta)}, \end{aligned} \quad (32)$$

which nicely simplifies to a pleasant homographic function of Y_m . Thus the function $\mu(\alpha)$ satisfies the nonlinear algebraic differential equation (32), which has unique solution $S_2(\alpha, \delta, \mu) = 0$. To select the convenient domains delimited by the intersection of the surfaces S_1 and S_2 , one can proceed by continuity with respect to parameters, starting for instance from a condition of the form $\mu = 2\alpha + \varepsilon$, for ε sufficiently small. Currently, we leave the details of this kind of bootstrapping as an open question.

VI. APPLICATION TO THE INTELLIGENT DRIVER MODEL

Although our results are usable with any local linearization of a car-following model of the form (1), it will be convenient to use the Intelligent Driver Model (IDM, see [17]), with the

TABLE I
PARAMETERS FOR THE IDM MODEL

Parameter	value
Desired velocity v_0	33 m/s
Safe time headway T	1.5 s
Maximum acceleration a	1.5 m/s ²
Desired deceleration b	1.5 m/s ²
Acceleration exponent δ	4
Jam distance s_0	2 m
Reaction time τ	1.5 s

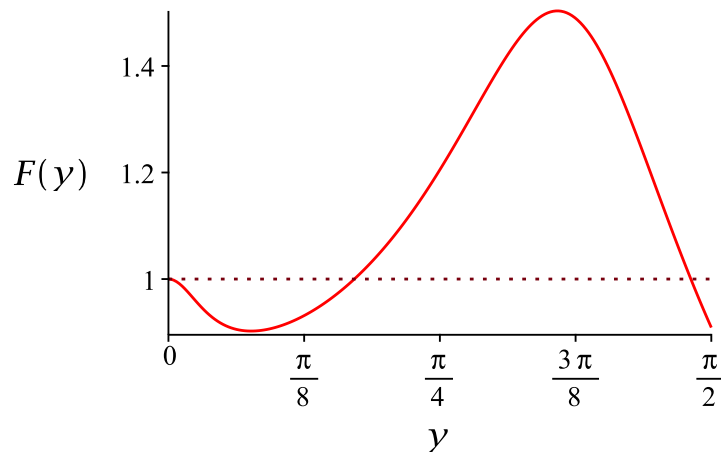


Fig. 4. Representation of the function $F(y) = |U(iy)|$ for the Intelligent Driver Model with parameters given in Table I and $v^* = 25$ m/s.

set of parameter given in Table I. As far as the reaction time is concerned, several studies suggest that the choice of $\tau = 1.5$ is quite reasonable, although the actual value depends on the circumstances [24], [25].

In order to see what happens on a particular example, let us pick an equilibrium speed $v^* = 25$ m/s. It is easy to solve explicitly the equilibrium equation (2), and find $\Delta x^* = 48.23$ m. Then the respective parameters of the linear system are $\alpha = 0.0975$, $\beta = 0.6366$ and $\gamma = 0.2332$. In this case $|U(iy)| \leq 1$ for $y \leq y_m = 0.5379$ and for $|U(iy)| > 1$ for $y_m < y < 1.5116$ (see Fig. 4).

Beyond the string stable and string unstable cases highlighted in [15], [16], the above example

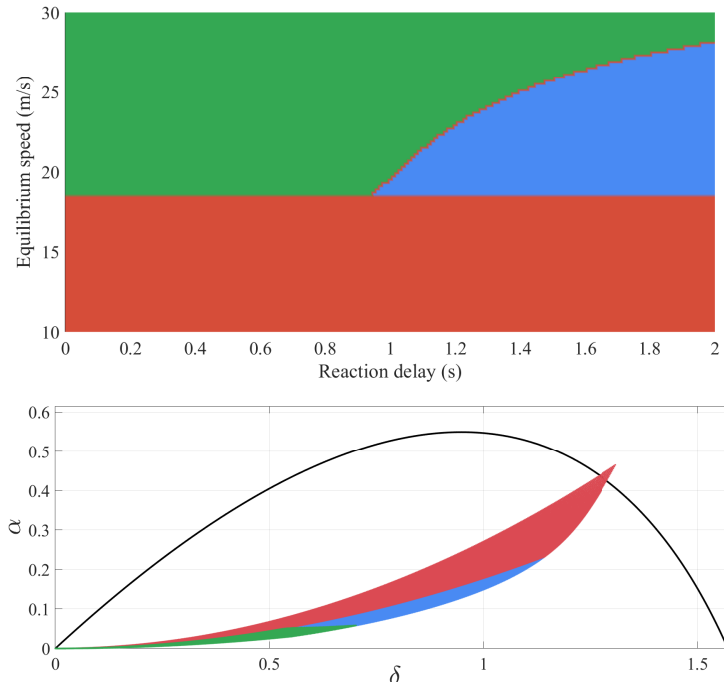


Fig. 5. Top: classification of string stability as a function of equilibrium speed v^* and reaction-time delay τ . Possible states are string stable (green), partially string stable (blue) and string unstable (red). Bottom: the same information set in the (δ, α) plane.

shows that introducing a reaction time can lead to an hybrid situation, which is string stable for values of y below some threshold.

More generally, it is possible to explore the parameter space of IDM by varying v^* and τ . The top graph of Fig. 5 shows the string stability classification of the linearized IDM depending on these parameters. As expected, the limit for string instability does not depend on τ . The same classification is shown in the bottom panel of Fig. 5 in the (δ, α) plane. For our chosen parameters of IDM, both full and partial string stability are clearly in the stability domain K_0 .

VII. CONCLUSION

As we have shown in this paper, the addition of a reaction time to some car-following models renders the analysis more intricate. Not only a nontrivial instability region appears, but in addition the string stability classification can be enriched by an intermediate class, referred to as *partial string stability*. This seems interesting because it permits new control strategies for string of vehicles, in particular when a few automated vehicles are inserted in a flow of human-driven

ones. Indeed, it becomes possible to take advantage of the range $|y| \leq y_c$, where $|U(iy)| \leq 1$, to regulate the amplification of potential shockwaves. This will be the focus of further research.

REFERENCES

- [1] Y. Sugiyama *et al.*, “Traffic jams without bottlenecks—experimental evidence for the physical mechanism of the formation of a jam,” *New Journal of Physics*, vol. 10, 2008.
- [2] R. E. Stern *et al.*, “Dissipation of stop-and-go waves via control of autonomous vehicles: Field experiments,” *Transportation Research Part C: Emerging Technologies*, vol. 89, pp. 205–221, 2018.
- [3] L. A. Pipes, “An operational analysis of traffic dynamics,” *Journal of Applied Physics*, vol. 24, no. 3, pp. 274–281, 1953.
- [4] R. E. Chandler, R. Herman, and E. W. Montroll, “Traffic dynamics: studies in car following,” *Operations research*, vol. 6, no. 2, pp. 165–184, 1958.
- [5] T. Toledo, “Driving behaviour: models and challenges,” *Transport Reviews*, vol. 27, no. 1, pp. 65–84, 2007.
- [6] P. G. Gipps, “A behavioural car-following model for computer simulation,” *Transportation Research Part B: Methodological*, vol. 15, no. 2, pp. 105–111, 1981.
- [7] M. Treiber, A. Hennecke, and D. Helbing, “Congested traffic states in empirical observations and microscopic simulations,” *Physical review E*, vol. 62, no. 2, p. 1805, 2000.
- [8] M. Treiber and D. Helbing, “Memory effects in microscopic traffic models and wide scattering in flow-density data,” *Physical Review E*, vol. 68, no. 4, p. 046119, 2003.
- [9] W. J. Schakel, B. Van Arem, and B. D. Netten, “Effects of cooperative adaptive cruise control on traffic flow stability,” in *Intelligent Transportation Systems (ITSC), 2010 13th International IEEE Conference on*. IEEE, 2010, pp. 759–764.
- [10] D. Helbing, “Traffic and related self-driven many-particle systems,” *Rev. Mod. Phys.*, vol. 73, pp. 1067–1141, Dec 2001. [Online]. Available: <https://link.aps.org/doi/10.1103/RevModPhys.73.1067>
- [11] A. Kesting and M. Treiber, “How reaction time, update time, and adaptation time influence the stability of traffic flow,” *Computer-Aided Civil and Infrastructure Engineering*, vol. 23, no. 2, pp. 125–137, 2008.
- [12] B. S. Kerner, *Breakdown in Traffic Networks. Fundamentals of Transportation Science*. Springer, 2017.
- [13] V. V. Kurtc and I. E. Anufriev, “Car-following model with explicit reaction-time delay: linear stability analysis of a uniform solution on a ring,” *Mathematical Models and Computer Simulations*, vol. 9, no. 6, pp. 679–687, Nov 2017.
- [14] M. Forster, R. Frank, M. Gerla, and T. Engel, “A cooperative advanced driver assistance system to mitigate vehicular traffic shock waves,” in *IEEE INFOCOM 2014 - IEEE Conference on Computer Communications*, April 2014, pp. 1968–1976.
- [15] S. Cui, B. Seibold, R. Stern, and D. B. Work, “Stabilizing traffic flow via a single autonomous vehicle: possibilities and limitations,” in *2017 IEEE Intelligent Vehicles Symposium (IV)*, June 2017, pp. 1336–1341.
- [16] C. Wu, A. Bayen, and A. Mehta, “Stabilizing traffic with autonomous vehicles,” in *IEEE Int. Conf. on Robotics and Automation*, 05 2018, pp. 1–7.
- [17] M. Treiber, A. Hennecke, and D. Helbing, “Congested traffic states in empirical observations and microscopic simulations,” *Phys. Rev. E*, vol. 62, pp. 1805–1824, 2000.
- [18] R. Bellman and K. L. Cooke, *Differential-Difference Equations*. New York: Academic Press, 1963.
- [19] E. Titchmarsh, *The Theory of Functions*, 2nd ed. Oxford University Press, New York, 1997.
- [20] M. Lavrentiev and B. Chabat, *Méthodes de la théorie des fonctions d’une variable complexe*, 2nd ed. Moscou: Mir, 1977.
- [21] R. M. Corless, G. H. Gonnet, D. E. G. Hare, D. J. Jeffrey, and D. E. Knuth, “On the Lambert W function,” *Advances in Computational Mathematics*, vol. 5, no. 1, pp. 329–359, 1996.

- [22] D. Swaroop and J. K. Hedrick, “String stability of interconnected systems,” *IEEE Transactions on Automatic Control*, vol. 41, no. 3, pp. 349–357, March 1996.
- [23] J. Ploeg, N. van de Wouw, and H. Nijmeijer, “ \mathcal{L}_p string stability of cascaded systems: Application to vehicle platooning,” *IEEE Transactions on Control Systems Technology*, vol. 22, no. 2, pp. 786–793, March 2014.
- [24] M. Green, ““How long does it take to stop?” Methodological analysis of driver perception-brake times,” *Transportation Human Factors*, vol. 2, no. 3, pp. 195–216, 2000.
- [25] D. V. McGehee, E. N. Mazzae, and G. H. S. Baldwin, “Driver reaction time in crash avoidance research: Validation of a driving simulator study on a test track,” *Proceedings of the Human Factors and Ergonomics Society Annual Meeting*, vol. 44, no. 20, pp. 3–320–3–323, 2000.



Guy Fayolle has been a researcher at Inria Paris since the early 1970s. He graduated from École Centrale in 1967 and obtained a Doctorat d’État ès-Sciences Mathématiques (Univ. Paris VI, Dept. of Probability, in 1979). He is currently Research Director Emeritus, member of the project-teams RITS and SPECFUN. His areas of interest are functional equations, random walks with boundaries, mathematical modeling of large complex systems (in particular telecommunication and transport networks), statistical physics (thermodynamic and hydrodynamic limits). He co-authored some 130 papers and two books.



analysis.

Jean-Marc Lasgouttes is a researcher at Inria Paris since 1996. He graduated from École Polytechnique in 1987 and obtained a PhD degree in Mathematics in 1995. He is interested in modeling large random systems, through the identification and development of solutions based on probabilistic methods and more specifically through the exploration of links between large random systems and statistical physics. Since he joined the RITS project-team, he applies these ideas to models related to ITS, both for macroscopic (fleet management, traffic prediction) and microscopic (movement of each vehicle, formation of traffic jams)



Carlos Flores received the B.Sc. degree in electronics engineering from Simón Bolívar University, Venezuela, in 2014. In 2018, he received the Ph.D. degree in the RITS Team, INRIA (Paris, France) and MINES ParisTech, PSL Research University (France). Since 2019, he is with California Partners for Advanced Transportation Technology, University of California Berkeley. His research interests include automated vehicles, cooperative driving and control of heterogeneous interconnected systems.